Heliyon 10 (2024) e32952

Contents lists available at ScienceDirect

Heliyon

journal homepage: www.cell.com/heliyon

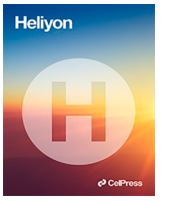

Research article

Atoh1 overexpression promotes Guinea pig bone marrow mesenchymal stem cells to differentiate into neural stem cell

Yiwen Chen [a], Ying Lin [a], Yuanhui Zhang [a], Xiaoping Liu [a], Ming Jiang [b,*]

[a] *Department of Otolaryngology Head and Neck Surgery, Guangzhou Red Cross Hospital (Guangzhou Red Cross Hospital of Jinan University), Guangzhou, Guangdong, 510240, China*
[b] *Department of Otolaryngology Head and Neck Surgery, The Third Xiangya Hospital of Central South University, Changsha, Hunan, 410013, China*

ARTICLE INFO

Keywords:
Bone marrow mesenchymal stem cells
Atoh1
Neural stem cells
Hair cell regeneration

ABSTRACT

Sensorineural hearing loss (SNHL) is a prevalent condition in otolaryngology. A key obstacle is finding effective strategies for regenerating damaged cochlear hair cells in adult animals. A practical and reliable approach has been developed to create a superior cell source for stem cell transplantation in the inner ear to treat SNHL. *Atoh1* is involved in the differentiation of neurons, intestinal secretory cells, and mechanoreceptors including auditory hair cells, and thus plays an important role in neurogenesis. Lentivirus-mediated transfection of bone marrow mesenchymal stem cells (BMSCs) was utilized to achieve stable expression of the essential transcription factor *Atoh1*, which is crucial for developing auditory hair cells without compromising cell survival. By manipulating the induction conditions through altering the cell growth environment using anti-adherent culture, the synergistic impact of basic fibroblast growth factor (bFGF) and epidermal growth factor (EGF) was effectively applied to significantly improve the differentiation efficiency of bone marrow-derived mesenchymal stem cells (BMSC) into neural stem cells (NSCs) following *Atoh1* transfection, thereby reducing the induction time. The study indicated that the newly proposed transdifferentiation method effectively transformed BMSCs into NSCs in a controlled environment, presenting a potential approach for stem cell transplantation to promote hair cell regeneration.

1. Introduction

Mesenchymal stem cells display tremendous promise in regenerative medicine. The investigators have utilized multiple kinds of mesenchymal stem cells, such as those from bone marrow, adipose tissue, and umbilical cord, to treat various clinical diseases. Several studies involving cell-based research have been conducted [1,2]. However, the development of stem cell therapy for sensorineural hearing loss is relatively lagging. Regenerating hair cells in the inner ear after their loss poses a challenge for otologists, hindering hearing recovery [3]. Current research on stem cell therapy for sensorineural hearing loss primarily centers on inducing specific differentiation conditions to transform stem cells from different tissues into inner ear precursor cells. These cells are subsequently delivered to the damaged areas and then migrate and perform physiological functions to improve hearing [4].

We have been especially interested in the ability of bone marrow-derived mesenchymal stem cells to develop into neural stem cells [5,6]. BMSCs can differentiate from mesoderm-derived cells to ectodermal cells. NSCs have the potential to differentiate into inner ear

* Corresponding author.
E-mail address: sallyzwkl@outlook.com (M. Jiang).

https://doi.org/10.1016/j.heliyon.2024.e32952
Received 17 February 2024; Received in revised form 6 June 2024; Accepted 12 June 2024
Available online 13 June 2024

sensory epithelium, as they share similar progenitor cell sources with the inner ear and central nervous system, both originating from the ectoderm. Research has demonstrated that NSCs can differentiate into inner ear hair-like cells in both vivo and in vitro [7,8]. These findings suggest that there is potential for Bone Marrow Stromal Cells(BMSCs) to transform into sensory epithelial cells in the inner ear.

Several transcription factors play a crucial role in hair cells' proliferation, differentiation, and development, with *Atoh1*, Gata3, Sox2, Gfi1, and Pou4f3 being particularly essential [9,10]. The *Atoh1* gene regulates inner ear development through various pathways. Inhibiting osteogenesis may raise *Atoh1* expression and hair cell production. The Notch pathway impacts sensory precursor cell differentiation by inhibiting *Atoh1* and activating the classical Wnt pathway, which can produce new hair cells, with *Atoh1* being a direct target of the Wnt pathway. It was determined that overexpressing the *Atoh1* gene could promote hair cells' regeneration and functional development [11–13]. This discovery reinforces the idea of overexpressing *Atoh1* in stem cells to transform them into functional inner ear hair cells.

Overall, this study facilitated the transfection of BMSCs with the *Atoh1* gene by overexpressing lentivirus, leading to sustained gene expression. This approach effectively accelerated the differentiation of BMSCs into NSCs under certain induction circumstances. Therefore, we investigated an innovative, quick, and secure approach to convert BMSCs into NSCs in a laboratory setting, which could offer an innovative idea and a superior cell supply for stem cell transplantation in the inner ear to address sensorineural hearing loss.

2. Material and methods

2.1. Laboratory animals and lentiviruses

2.1.1. Materials

The LV-Atoh1-gcGFP vector was provided by Gikai Gene. DMEM and DMEM/F12 media were purchased from GIBCO (NY, USA) and Biosharp (Guangzhou, China), respectively. Antibodies used included PE anti-mouse CD45, FITC anti-rat CD29, and PE anti-rat CD90 (BD Biosciences, CA, USA), Math1 (GeneTex, Texas, USA), and Nestin (Cell Signaling Technology, MA, USA). Secondary antibody, Goat anti-mouse IgG (H + L) Cy3, was from Proteintech (Beijing, China). Real-time PCR kit and TRIZOL were from TransGen Biotech (Beijing, China). EGF and bEGF were supplied by PeproTech (NJ, USA). The CCK-8 assay kit and Alizarin red S staining kit were obtained from Beyotime (Shanghai, China). Neural supplements B27, N2, Alcian blue solution, and Oil red O stain kit were sourced from Solarbio (Beijing, China).

2.1.2. Laboratory animals

All animal procedures were carried out in strict accordance with the ethical guidelines of the Regulations of the People's Republic of China on the Administration of Laboratory Animals. The protocol was approved by the Animal Care and Use Committee of Central South University (Approval No. T22037). Male guinea pigs, 2 weeks old and weighing approximately 150 g, were obtained from the Department of Experimental Animal Science at Central South University. Prior to the experiments, all animals were acclimatized under optimal conditions to ensure good health.

2.2. Isolation, culture, identification, and trilineage induction of Guinea pig BMSCs

2.2.1. Isolation and culture of Guinea pig BMSCs

Guinea pigs were anesthetized and disinfected, and the humerus and femur were separated. The distal femur and proximal tibia were cut off to expose the bone marrow cavity. The bone marrow cavity was rinsed at the broken end with DMEM medium (10 % FBS, 100 U/mL penicillin, and 100 μg/mL streptomycin) 4–5 times. The bone marrow cell suspension was collected and uniformly spread into cell culture plates at an appropriate density and cultured in a constant temperature incubator and the cells were labeled P0. The growth and attachment of the primary cells were regularly observed under an inverted microscope. Half of the media was changed for the first time after 24 h, and the whole media volume was changed after 48 h. The solution was then changed once every three days. When cells reached approximately 80 %–90 % confluence, they were detached using trypsin digestion. As soon as adherent cells started exhibiting signs of cytoplasmic retraction, cell roundness, and enlarged intercellular spaces, the digestion was terminated by adding DMEM medium containing FBS. To separate clumped cells into individual cells, the cell mass was gently agitated using a Papanicolaou straw. The cells were divided for passage and the third generation of BMSC cells (P3) were selected for the experiment.

2.2.2. Identification of surface markers of BMSCs

Cell suspensions were prepared at a concentration of 2×10^6 cells/mL. For each antibody (FITC-CD29, PE-CD45, PE-CD90), 5 μL was added to separate 1.5 mL centrifuge tubes, with three replicates per antibody. A negative control was also established. The tubes were incubated at 4 °C in the dark. After incubation, each tube received 1 mL of PBS and was centrifuged at 2000 rpm for 10 min to remove excess antibodies. The supernatant was discarded, and the cell pellet was resuspended in 0.5 mL of PBS. The expression of the cell surface markers CD29, CD45, and CD90 was assessed using flow cytometry. Data were analyzed using CellQuest software. All experiments were conducted in triplicate.

2.2.3. Verification of the potential of the primary BMSCs to induce three lineages

2.2.3.1. Osteogenesis induction and alizarin red staining of BMSCs. Osteogenic induction system was configured: 100 nM

dexamethasone, 50 μM ascorbic acid-2-phosphate, 10 mM sodium β-glycerophosphate, 10 mL FBS, 1 mL of bispecific antibody mixed with DMEM, and 100 mL of fixed volume for later use. P3 BMSCs was seeded in a 6-well plate with BMSCs of 3×10^5 cells, and when the cells reached 60 %~80 % confluency, the complete medium was replaced with the above induction medium.

The medium of the osteogenic induction system was changed every 48–72 h. It was aspirated and discarded at 21–28 days, washed with PBS, fixed with 4 % paraformaldehyde for 15 min, and then subjected to alizarin red staining and microscopic observation.

2.2.3.2. Pellet method for BMSCs into cartilage-induced differentiation and alcian blue staining. Configured into a cartilage induction system: ITS additives (0.5 mg bovine insulin, 0.24 mg linolenic acid, 0.25 μg sodium selenite, 225 μg human transferrin), 5 mg sodium pyruvate, 2 mg L-proline, 0.05 mg TGF-β3, 0.05 μM dexamethasone, 2.5 mL L-ascorbic acid-2-phosphate. Then, use serum-free DMEM to 100 mL at 4 °C for later use.P3 BMSCs, move to a 15 mL centrifuge tube with BMSCs of 3×10^5 cells, and centrifuge at 250g for 4min. To remove the supernatant, add 500 μL of chondrogenic induction system medium to resuspend, centrifuge at 150g for 5min, and repeat 3 times.

Transfer to 37 °C, 5 % CO2 incubator, loosen the mouth of the centrifuge tube slightly, facilitate gas exchange, stand for 48h to observe the bottom of the tube, flick the bottom of the tube when there is a cluster of cell clumps, make the clumps disperse and suspension, change the liquid every 48h–72h, and when the induction is about 21–28 days, take 4 % paraformaldehyde and fix it for 30 min, perform follow-up Alcian blue staining, and observe under an inverted microscope.

2.2.3.3. Adiposogenic induction and oil red O staining of BMSCs. Configure the lipid induction system: 1 mg insulin, 0.05mol IBMX (1-methyl-3-isobutylexanthine), 0.1 mM dexamethasone, add to DMEM containing 10 % FBS and 1 % bispecific antibody, and set the volume to 100 mL.

P3 BMSCs with 3×10^5 cell amount were seeded in 6-well plates, and when the cells were confluent to more than 60 %, they were completely cultured and 2 mL of adipogenesis induction system was added; Half-feed every 48 h for a total of 18–21 days; After the induction was completed, the medium was aspirated, the PBS was rinsed twice and then fixed with 4 % paraformaldehyde, the oil red O staining solution was used for 20 min and then discarded, and the plate was cleaned with PBS for 2 times, and the microscope was observed.

2.3. Lentivirus-mediated infection of Guinea pig BMSCs with the Atoh1 gene and verification of expression

2.3.1. Lentivirus-mediated Atoh1 gene infection of BMSCs and observations

Lentivirus nuclear transcription factor Atoh1-strong green fluorescent protein (LV-Atoh1-GC GFP) for infection of BMSCs: P3 cells were added to 96-well plates (1×10^6/well). The P3 BMSCs were divided into three groups; the Trial group (BMSCs + lentivirus overexpressing *Atoh1* gene), the NC group (BMSCs + empty lentivirus), and the Blank group (uninfected BMSCs). The multiplicity of infection (MOI) value of the optimal infection efficiency was determined (note: according to the preliminary experimental results, MOI was assumed to be 10). The medium of the three groups was changed after 24 h of culture, and the expression of the reporter gene gcGFP was observed under the fluorescence microscope 72 h after infection. The total cells from five random fields and the cells with strong fluorescence were selected to calculate the transfection efficiency.

2.3.2. Detection of Atoh1 mRNA expression by RT-PCR

The Trial and the NC groups were infected with the virus for three days. The cultured cells of the three groups were harvested and 1 mL Trizol reagent was added at room temperature for 5 min to fully lyse the cells. The total RNA in cells was extracted using the chloroform method, and the RNA concentration was measured with a micro-spectrophotometer. After 1.0 μg of total RNA was reverse transcribed, the expression of *Atoh1* mRNA in the three groups of cells was detected by real-time PCR using the TransStart Real-time PCR kit with rat *Gapdh* as the internal reference and the ABI 7500 real-time fluorescent quantitative PCR instrument. Upstream primer: GTCTACCCGGCAGAACTGTC; Downstream primer: AGTTGTTCCCGCACTTTCAC. Reaction conditions: 95 °C 3 min preheating, 95 °C 30s, 55 °C 20s, 72 °C 20s, 40 cycles. The experiment was repeated three times.

2.3.3. Detection of expression of ATOH1 protein by Western blot

Protease inhibitors PMSF and AEBFS cocktail, Triton-100, and $NaVO_3$ were added to the basic lysis solution. After the Trial and the NC groups were infected with the virus for seven days, proteins were harvested from all three groups of cells and analyzed using the Beyotime BCA protein concentration determination kit. After SDS-PAGE electrophoresis separation and transmembrane transfer, the PVDF membranes were immersed in primary antibody incubation solution and shaken at 4 °C overnight. The blot was thoroughly washed to remove the primary antibody and the PVDF membrane was immersed in the HRP-labeled secondary antibody incubation solution for 2 h. After development, the grayscale of the band was analyzed using Image J software. Three samples were taken from each group, and the experiment was repeated three times for each sample.

2.4. In vitro induction of BMSCs transdifferentiation into neural stem cells

2.4.1. Induced BMSCs into neural stem cells and observation

BMSCs in the above three groups were selected for good growth state, and, where appropriate, high virus transfection rate, fewer deaths after virus infection, and intense proliferation. When the fusion rate of long spindle cells was close to 50 %–60 %, trypsin was

used to digest and re-suspend the cells which were then adjusted to the appropriate concentration (4×10^6/mL). Cells from the Trial and NC groups were inoculated into agar-coated cell culture plates (T100), while the Blank group cells were inoculated into empty plates (T100). The cells from each of the three groups were distributed for transdifferentiation culture according to the following culture conditions, 50 mL DFNB basic induction medium + 1 mL EGF (20 ng/mL) + 1 mL bFGF (20 ng/mL). The DFNB basic induction medium was prepared by DMEM/F12, B27, and N2 (the volume ratio was 100:2:1), and mixed evenly after adding 1 % cyan-streptomycin bispecific antibody. The medium was changed once every three days depending on the color change of the medium. The morphological changes of the cells were observed under a fluorescence microscope 1, 5, and 7 days after induction transformation culture and were recorded.

2.4.2. *Detection of cell proliferation with the CCK-8 method*

Cells from the Trial group and NC group were inoculated into agar-coated 96-well culture plates with the appropriate concentration (4×10^4/mL), while the Blank group cells were inoculated into empty plates, induced, and cultured according to the above conditions. The OD 450 value was measured on days 0, 3, and 5 with a microplate reader, then the proliferation curve was recorded and plotted.

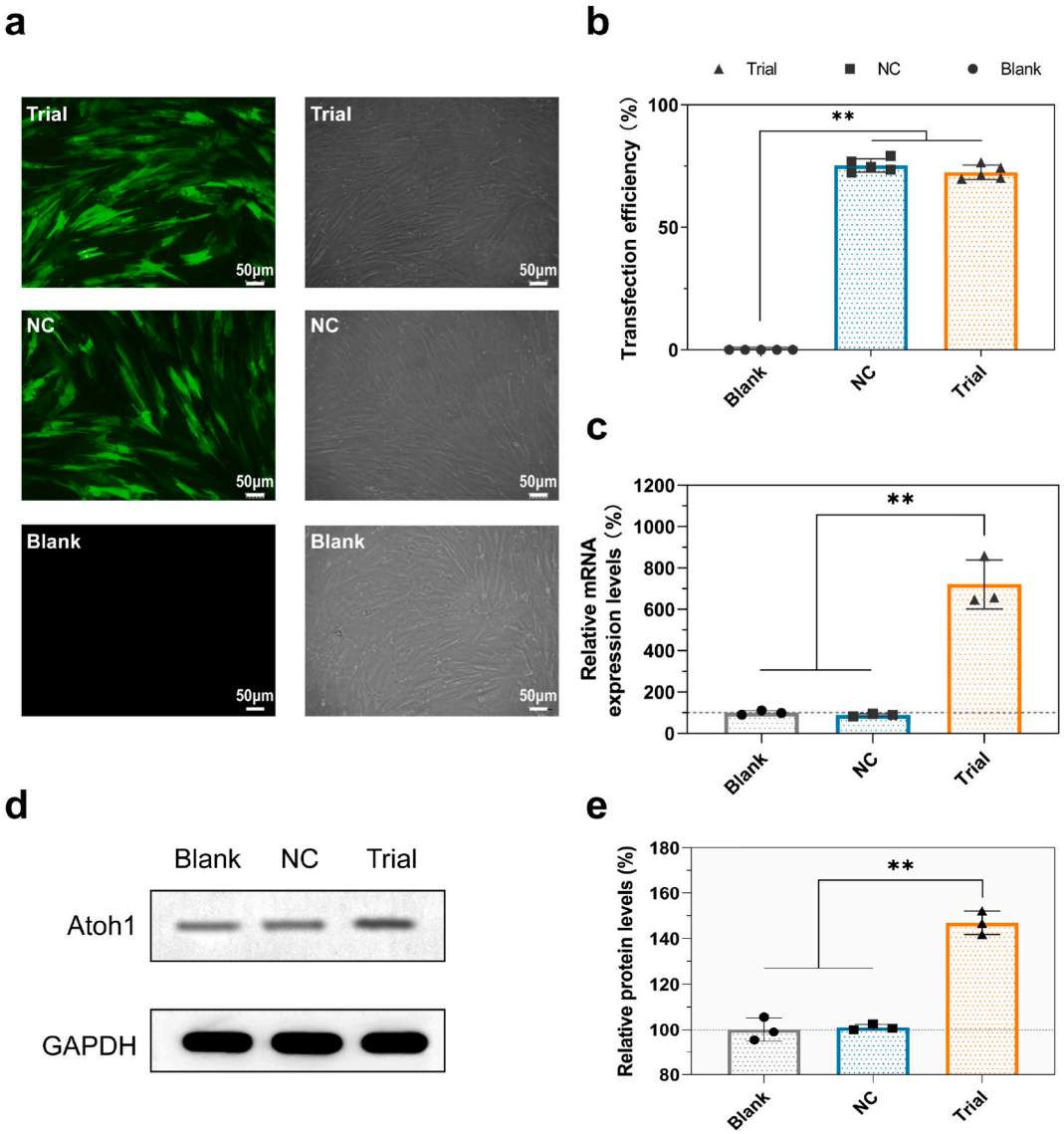

Fig. 1. Expression of lentivirus overexpressing *Atoh1* gene after infection with BMSCs. (a) Morphological findings of BMSCs infected by lentivirus overexpressing *Atoh1* gene. All scale bars: 50 μm. **(b)** Infection efficiency of lentivirus overexpressing *Atoh1*. $^*p < 0.05$,$^{**}p < 0.01$,$n = 5$. **(c)** Expression of *Atoh1* mRNA in BMSCs infected with lentivirus. $^*p < 0.05$,$^{**}p < 0.01$,$n = 3$. **(d–e)** Expression of ATOH1 protein in BMSCs infected with lentivirus and WB strip. $^*p < 0.05$,$^{**}p < 0.01$,$n = 3$. The data obtained from the above experiments are expressed as mean and standard deviation. One-way ANOVA followed by Tukey's post hoc test was used for statistical analysis.

2.4.3. Immunofluorescence detection of nestin expression after BMSCs transdifferentiation into NSCs

Cells from the Trial group and NC group were inoculated into agar-coated 24-well culture plates with the appropriate concentration (2.5×10^5/mL), while the Blank group cells were inoculated into empty plates, induced, and cultured according to the above conditions. The time of plating was recorded as 0 days beginning after a 4-h stabilization period. Immunofluorescence staining was performed after the cells were fixed on the third day. Before all cells are fixed with 4 % paraformaldehyde, it is worth noting that the cells in the Trial and NC groups need to be made into cell smears for subsequent manipulation because they are not adherent to the wall. Cells were then permeabilized with 1 % Triton-X-100, blocked with 5 % BSA for 30min, and incubated with primary antibody (1:100) overnight at 4 °C. Secondary antibodies (Goat Anti-Mouse IgG (H + L) Cy3 (1:100)) were incubated for 2 h at 37 °C. After being washed with PBS in a dark environment, DAPI stain was added for 10 min. Followed by observation and photographing under a fluorescence microscope.

2.5. Statistical analysis

The data obtained from the above experiments are expressed as mean and standard deviation(SD). One-way ANOVA followed by Tukey's post hoc test was used for statistical analysis. All data were analyzed using GraphPad Prism 9.5.1 software. (*$p < 0.05$ significant, * *$p < 0.01$ very substantial).

3. Results

3.1. Culture and identification of BMSCs

Bone Marrow Stromal Cells were isolated using the whole bone marrow adherent technique. Once the cells acquired 80 %–90 % confluence, they were subcultured. The cells usually grow elongated and spindle-shaped by the third generation, arranged in a swirling pattern. Cells revived following cryopreservation maintain comparable morphological and growth traits but with a slightly slower growth rate (Fig. S1a). Flow cytometry was utilized to identify BMSCs by detecting the positive expression of CD29, CD45, and CD90. The results were presented in Fig. S1b and Table S1, indicating that the average expression levels of CD29, CD45, and CD90 were 95.93 %, 5.60 %, and 97.67 %, respectively.

The staining results of alizarin red after osteogenic induction of differentiation of BMSCs are shown in Fig. S2a, and a large area of cells is colored red under the microscope, indicating that alizarin red dye forms chelates with intracellular calcium salts and mineralized nodules are formed. The Pellet method showed that intracellular chondroitin sulfate binds to the alcian blue basic group, suggesting that cartilage induction can differentiate the extracted BMSCs into chondrocytes (Fig. S2b). Oil Red O staining showed that the dye was successfully immersed into the lipid droplets, indicating that the extracted BMSCs had adipogenic differentiation potential (Fig. S2c).

3.2. Lentivirus expressing the Atoh1 gene infection of BMSCs and validation of Atoh1 gene expression

3.2.1. Observation of lentivirus-mediated infection of BMSCs with the Atoh1 gene

The appropriate multiplicity of infection (MOI) was determined by counting the total number of cells in five fields and the number of cells exhibiting strong fluorescence after 72 h of lentivirus infection in cells (Fig. 1a). The transfection efficiencies of the Trial and NC groups have been calculated to be 72.42 ± 1.31 % and 75.28 ± 1.21 % (Fig. 1b). The transfection efficiency of the Trial and NC groups was considerably higher than that of the Bank group ($p < 0.01$).

3.2.2. Determination of the expression level of Atoh1 mRNA by RT-PCR

The experimental results were analyzed by the comparative CT method, and the relative expression level of the target gene was equal to $2^{-\Delta\Delta CT}$. Then, the relative expression levels of the target gene ($2^{-\Delta\Delta CT}$) in the Trial group, the NC group, and the Blank group were 7.17 ± 0.38 %, 0.89 ± 0.02 %, and 1.00 ± 0.10 %, respectively. Compared with the NC and Blank group, the expression of *Atoh1* mRNA in the Trial group was significantly higher (**$p < 0.01$). In contrast, there was no explicit distinction between the NC and Blank groups. These results revealed that the lentivirus-mediated *Atoh1* gene could successfully infect the third generation of guinea pig BMSCs in vitro and express *Atoh1* mRNA (Fig. 1c).

3.2.3. Determination of ATOH1 protein expression by Western blot

The Western Blot was conducted thrice to determine the relative protein expression levels of the *Atoh1* protein in each group. The results imply that the *Atoh1* protein expression in the NC and Blank groups was lower than in the Trial group (**$p < 0.01$), as shown in Fig. 1e. The results showed effective transfection of the lentivirus-mediated *Atoh1* gene into third-generation guinea pig BMSCs in vitro, leading to the expression of the *Atoh1* protein (Fig. 1d).

3.3. Observation of induction of BMSCs transformation to NSCs and determination of the expression result of NSC marker nestin

During the initial day of BMSCs-induced transformation, the Trial and NC groups presented a limited amount of spheroid changes and were diminutive. Conversely, the growth condition of BMSCs in the Blank group remained unchanged. Fluorescence expression occurred in the Trial and NC groups under the fluorescence microscope while absent in the Blank group. On the 3rd and 5th day after

induction, there was notable cytoplasmic retraction of cells in both the Trial and NC groups. Most cells transformed into neural balls, increased size, and lost their adhesion properties. The cells in the Blank group remained adhered to and continued to proliferate in that condition. Under the fluorescent microscope, strong fluorescence expression was observed in both the Trial and NC groups. On the 7th day post-induction, the cells in the Trial and NC groups began undergoing apoptosis, whereas the cell proliferation in the Blank group remained unaffected (Fig. 2).

3.3.1. *Results of cell proliferation detected by CCK-8 method*

The CCK-8 approach was utilized to assess cell proliferation and survival in three groups at 0, 3, and 5 days post-induction. The results were presented in Fig. 3a, demonstrating no substantial variation in cell survival rates among the three groups on Day 0 and Day 3. But on the 5th days after induction, the Trial group displayed a substantial rise in cell proliferation rate compared to the Blank and the NC group ($^*p < 0.05$). This illustrated that overexpressing the *Atoh1* gene might boost the proliferation and differentiation of BMSCs.

3.3.2. *Detection by immunofluorescence of nestin expression after BMSCs induction into NSCs*

Immunofluorescence showed that on the third day after BMSCs induced NSCs, the expression of Nestin in the neuroglobular cells formed in the Trial group was markedly increased compared to the NC group or the Blank group. The nestin expression is located in the nucleus and is consistent with DAPI nuclear staining (Fig. 3c). Nestin expression in the neural balls was modest in the NC group, whereas there was minimal Nestin expression in the Blank group (Fig. 3b). Based on the immunofluorescence data and observed

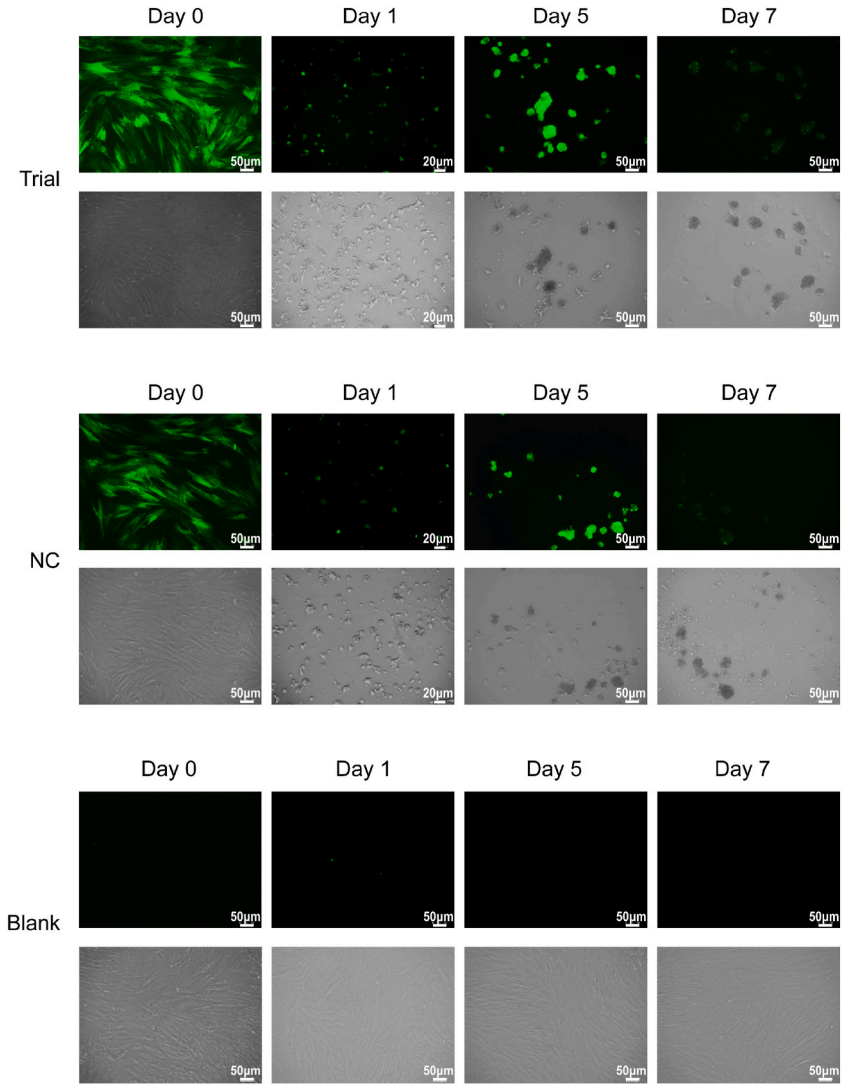

Fig. 2. Morphological findings on different days after subgroup induction of BMSCs into NSCs. Scale bars: Trial-D1, NC-D1, 20 μm, others, 50 μm.

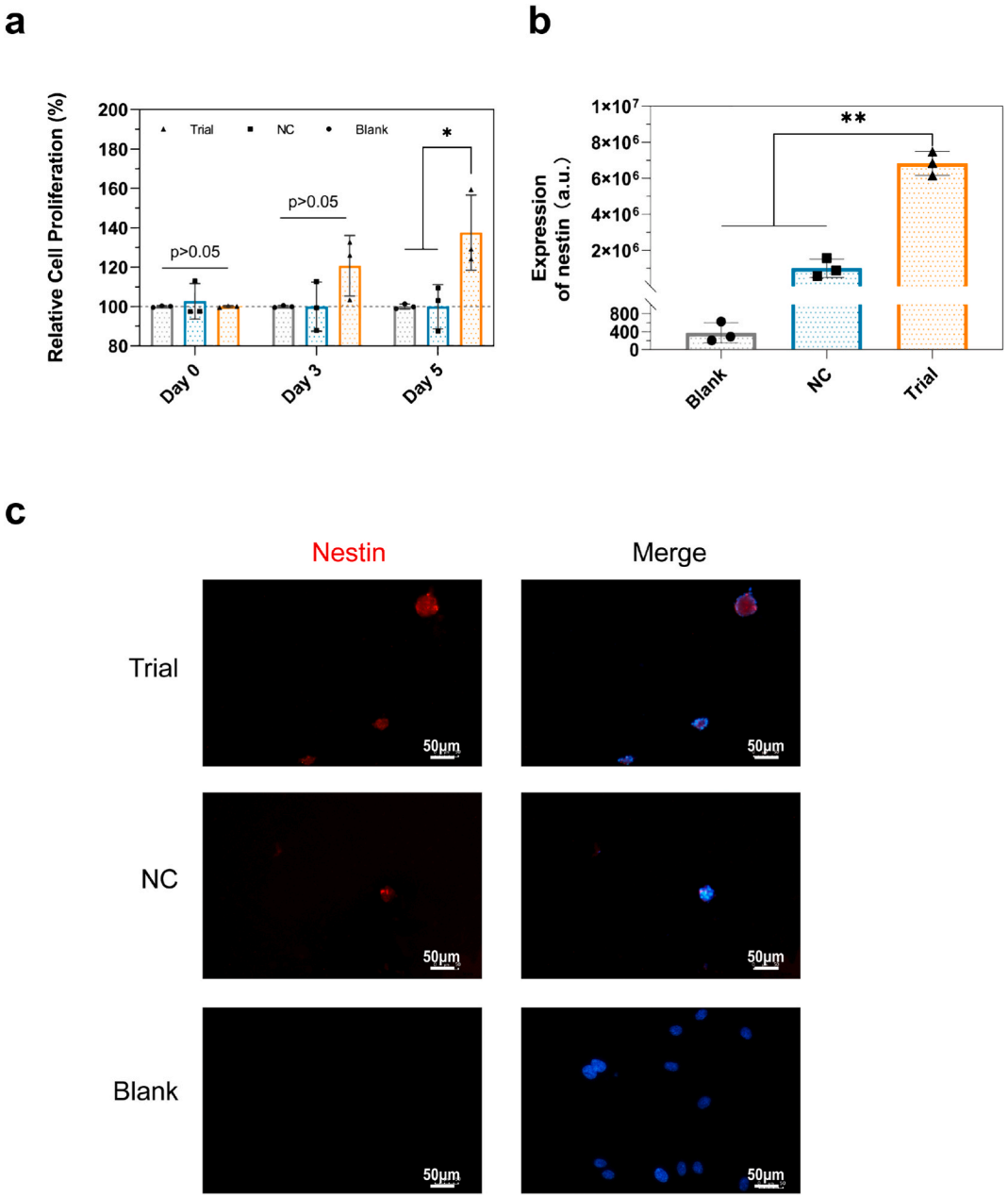

Fig. 3. CCK-8 detection and immunofluorescence results after BMSCs induction to NSCs. (a) Cell proliferation on different days after BMSCs induction to NSCs. **(b)** Quantitative analysis of the nestin. **(c)** Immunofluorescence results of Nestin after bone marrow mesenchymal stem cells are induced into NSCs. All scale bars: 50 μm. The data obtained from the above experiments are expressed as mean and standard deviation. One-way ANOVA followed by Tukey's post hoc test was used for statistical analysis. $*p < 0.05$,$**p < 0.01$,$n = 3$.

morphological alterations, it was hypothesized that the cells in the Trial group might transform into NSCs in vitro.

4. Discussion

Bone marrow mesenchymal stem cells have grown in popularity in the field of regeneration due to their multiple origins, being accessible to extract, proliferating well, and having minimal immunogenicity [1,14]. Modifying the surroundings of bone marrow mesenchymal stem cell culture or introducing alternative growth factors by vector transfection could potentially enhance the differentiation of BMSCs into cochlear hair cells. The research reports that viral vectors typically exhibit superior transfection effectiveness compared to non-viral vectors and electroporation transfection [15,16]. Viral vectors can efficiently transfect the target gene,

alter its expression through overexpression or repression, and integrate the foreign gene into the target cell genome [17].

Adenovirus transgenes feature a shorter and quicker peak effective expression duration than lentivirus [18,19]. In this experiment, lentiviral vectors carrying target genes were chosen to transfer into BMSCs, taking into account the growth characteristics and survival time of BMSCs. The lentivirus showed the highest activity between 72 and 120 h after being introduced into BMSCs, aligning with the expected transfection properties of lentivirus [20,21]. Thus, our group decided to measure gene expression 72 h post-transfection.

bFGF is a cytokine with a broad spectrum of effects on nerve growth and cell division. It not only stimulates stem cell regeneration but also influences how stem cells develop into different cell types. EGF is a peptide that controls cell growth and specialization. It helps inner ear progenitor cells develop into hair cells, but hair cells in the inner ear cannot mature without EGF stimulation. The combined effect of bFGF and EGF in promoting the transformation of BMSCs into neural stem cells was more effective than other growth factors [22,23]. Extracellular matrix and culture conditions influence stem cell differentiation direction [24]. Agar is a cell wall component abundant in minerals, carbohydrates, sulfates, and calcium, and it can absorb water. Choosing a specific agar covering can alter the growth conditions for BMSCs, leading to cytoplasmic retraction, faster transdifferentiation, and the formation of cells with neurospheroid features.

Nestin, an intermediate silk protein, is a known marker for NSCs found in murine and human inner ear progenitor cells [25,26]. Thus, transforming BMSCs into NSCs in a lab setting could be a crucial step in the differentiation process to become cells resembling inner ear hair cells. The study showed that the proliferation of BMSCs into neural stem cells peaked within the first 3–5 days following transdifferentiation. Immunofluorescence cell labeling revealed a substantial increase in Nestin expression in the Trial group compared to the NC and Blank groups. Cell morphology revealed no significant distinction between the Trial and NC groups. However, there was an apparent variance in Nestin expression, a marker of NSCs. This implies that overexpressing the *Atoh1* gene facilitated the conversion of BMSCs into NSCs in vitro without impacting cell morphology or biological traits [27].

During the transdifferentiation culture stage, it was observed that neurospheroid cells' viability and apoptosis decreased over time. Introducing agar packs to change the culture environment and speed up the transformation of BMSCs into NSCs may negatively impact their growth mechanism. To ensure the continued differentiation of NSCs into hair cells, the culture environment should be promptly modified after introducing foreign genes to extend the survival period of stem cells.

5. Conclusion

This study effectively transfected BMSCs with the *Atoh1* gene using a lentivirus-mediated system, leading to its stable overexpression confirmed by RT-PCR and Western blot analysis. Optimized induction culture conditions successfully reduced the differentiation time of BMSCs into NSCs. Enhanced proliferative activity in *Atoh1*-overexpressing BMSCs was verified using the CCK-8 assay. Furthermore, immunofluorescence staining demonstrated increased transdifferentiation efficiency into neural stem cells and superior expression of the NSC marker, Nestin, in these cells. These findings suggest the potential for in vitro differentiation of BMSCs into inner ear hair cell-like cells, opening avenues for regenerative therapies in auditory research.

Funding

This work was supported by the Nature and Science Foundation of Hunan Province (06jj50066), Nanopore sequencing for prevention and controlling congenital hearing loss (2023A03J0520), Guangzhou Key Laboratory of Clinical and Basic Research, Otolaryngology Department (2023A03J0521) and Guangzhou Clinical High-tech Project (2023C-GX05).

Data availability statement

The data that support the findings of this study are available from the corresponding author upon reasonable request.

CRediT authorship contribution statement

Yiwen Chen: Writing – original draft, Validation, Formal analysis, Data curation, Conceptualization. **Ying Lin:** Data curation, Methodology, Resources, Software. **Yuanhui Zhang:** Investigation, Formal analysis. **Xiaoping Liu:** Investigation. **Ming Jiang:** Writing – review & editing, Supervision, Project administration, Funding acquisition, Formal analysis, Conceptualization.

Declaration of competing interest

The authors declare that they have no known competing financial interests or personal relationships that could have appeared to influence the work reported in this paper.

Appendix A. Supplementary data

Supplementary data to this article can be found online at https://doi.org/10.1016/j.heliyon.2024.e32952.

References

[1] H. Lin, H. Chen, X. Zhao, Z. Chen, P. Zhang, Y. Tian, Y. Wang, T. Ding, L. Wang, Y. Shen, Advances in mesenchymal stem cell conditioned medium-mediated periodontal tissue regeneration, J. Transl. Med. 19 (2021) 456, https://doi.org/10.1186/s12967-021-03125-5.

[2] H. Jo, S. Brito, B.M. Kwak, S. Park, M.-G. Lee, B.-H. Bin, Applications of mesenchymal stem cells in skin regeneration and rejuvenation, Int. J. Mol. Sci. 22 (2021) 2410, https://doi.org/10.3390/ijms22052410.

[3] J. Qi, W. Huang, Y. Lu, X. Yang, Y. Zhou, T. Chen, X. Wang, Y. Yu, J.-Q. Sun, R. Chai, Stem cell-based hair cell regeneration and therapy in the inner ear, Neurosci. Bull. 40 (2024) 113–126, https://doi.org/10.1007/s12264-023-01130-w.

[4] J. Wang, J. Zheng, H. Wang, H. He, S. Li, Y. Zhang, Y. Wang, X. Xu, S. Wang, Gene therapy: an emerging therapy for hair cells regeneration in the cochlea, Front. Neurosci. 17 (2023) 1177791, https://doi.org/10.3389/fnins.2023.1177791.

[5] H. Qin, L.-D. Zhao, J.-H. Sun, L.-L. Ren, W.-W. Guo, H.-Z. Liu, S.-Q. Zhai, S.-M. Yang, The differentiation of mesenchymal stem cells into inner ear hair cell-like cells in vitro, Acta Otolaryngol. 131 (2011) 1136–1141, https://doi.org/10.3109/00016489.2011.603135.

[6] F. Shi, J.S. Kempfle, A.S.B. Edge, Wnt-responsive Lgr5-expressing stem cells are hair cell progenitors in the cochlea, J. Neurosci. 32 (2012) 9639–9648, https://doi.org/10.1523/JNEUROSCI.1064-12.2012.

[7] K. Kojima, S. Tamura, A.T. Nishida, J. Ito, Generation of inner ear hair cell immunophenotypes from neurospheres obtained from fetal rat central nervous system in vitro, Acta Otolaryngol Suppl (2004) 26–30, https://doi.org/10.1080/03655230310016762.

[8] X.-W. Liu, J.-W. Sun, Primary culture of neurospheres obtained from fetal mouse central nervous system and generation of inner ear hair cell immunophenotypes in vitro, J. Laryngol. Otol. 125 (2011) 686–691, https://doi.org/10.1017/S0022215110002914.

[9] C. Zhong, Y. Fu, W. Pan, J. Yu, J. Wang, Atoh1 and other related key regulators in the development of auditory sensory epithelium in the mammalian inner ear: function and interplay, Dev. Biol. 446 (2019) 133–141, https://doi.org/10.1016/j.ydbio.2018.12.025.

[10] Y. Hayashi, H. Chiang, C. Tian, A.A. Indzhykulian, A.S.B. Edge, Norrie disease protein is essential for cochlear hair cell maturation, Proc Natl Acad Sci U S A 118 (2021) e2106369118, https://doi.org/10.1073/pnas.2106369118.

[11] D. You, W. Ni, Y. Huang, Q. Zhou, Y. Zhang, T. Jiang, Y. Chen, W. Li, The proper timing of Atoh1 expression is pivotal for hair cell subtype differentiation and the establishment of inner ear function, Cell. Mol. Life Sci. 80 (2023) 349, https://doi.org/10.1007/s00018-023-04947-w.

[12] H. Gálvez, J.J. Tena, F. Giraldez, G. Abelló, The repression of Atoh1 by Neurogenin1 during inner ear development, Front. Mol. Neurosci. 10 (2017) 321, https://doi.org/10.3389/fnmol.2017.00321.

[13] E.C. Driver, M.W. Kelley, Development of the cochlea, Development 147 (2020) dev162263, https://doi.org/10.1242/dev.162263.

[14] P. Charbord, Bone marrow mesenchymal stem cells: historical overview and concepts, Hum. Gene Ther. 21 (2010) 1045–1056, https://doi.org/10.1089/hum.2010.115.

[15] T.K. Kim, J.H. Eberwine, Mammalian cell transfection: the present and the future, Anal. Bioanal. Chem. 397 (2010) 3173–3178, https://doi.org/10.1007/s00216-010-3821-6.

[16] M.A. Schmitt, O. Friedrich, D.F. Gilbert, Portoporator©: a portable low-cost electroporation device for gene transfer to cultured cells in biotechnology, biomedical research and education, Biosens. Bioelectron. 131 (2019) 95–103, https://doi.org/10.1016/j.bios.2019.02.024.

[17] S. Ramani, S.E. Crawford, S.E. Blutt, M.K. Estes, Human organoid cultures: transformative new tools for human virus studies, Curr Opin Virol 29 (2018) 79–86, https://doi.org/10.1016/j.coviro.2018.04.001.

[18] Q. Zeng, Y. Zhou, D. Liang, H. He, X. Liu, R. Zhu, M. Zhang, X. Luo, Y. Wang, G. Huang, Exosomes secreted from bone marrow mesenchymal stem cells attenuate oxygen-glucose deprivation/reoxygenation-induced pyroptosis in PC12 cells by promoting AMPK-dependent autophagic flux, Front. Cell. Neurosci. 14 (2020) 182, https://doi.org/10.3389/fncel.2020.00182.

[19] L. Zhang, Q. Wei, X. Liu, T. Zhang, S. Wang, L. Zhou, L. Zou, F. Fan, H. Chi, J. Sun, D. Wang, Exosomal microRNA-98-5p from hypoxic bone marrow mesenchymal stem cells inhibits myocardial ischemia-reperfusion injury by reducing TLR4 and activating the PI3K/Akt signaling pathway, Int Immunopharmacol 101 (2021) 107592, https://doi.org/10.1016/j.intimp.2021.107592.

[20] Z. Wu, J. Zhu, Y. Wen, P. Lei, J. Xie, H. Shi, R. Wu, X. Lou, Y. Hu, Hmga1-overexpressing lentivirus protects against osteoporosis by activating the Wnt/β-catenin pathway in the osteogenic differentiation of BMSCs, FASEB J 37 (2023) e22987, https://doi.org/10.1096/fj.202300488R.

[21] R.A. Torres-Guzman, F.R. Avila, K.C. Maita, J.P. Garcia, G.D. De Sario, S. Borna, A.S. Eldaly, A. Quinones-Hinojosa, A.C. Zubair, O.A. Ho, A.J. Forte, Bone morphogenic protein and mesenchymal stem cells to regenerate bone in calvarial defects: a systematic review, J. Clin. Med. 12 (2023) 4064, https://doi.org/10.3390/jcm12124064.

[22] M. Xu, X. Wei, J. Fang, L. Xiao, Combination of SDF-1 and bFGF promotes bone marrow stem cell-mediated periodontal ligament regeneration, Biosci. Rep. 39 (2019) BSR20190785, https://doi.org/10.1042/BSR20190785.

[23] S. Niknazar, H.-A. Abbaszadeh, H. Peyvandi, O. Rezaei, H. Forooghirad, S. Khoshsirat, A.A. Peyvandi, Protective effect of [Pyr1]-apelin-13 on oxidative stress-induced apoptosis in hair cell-like cells derived from bone marrow mesenchymal stem cells, Eur. J. Pharmacol. 853 (2019) 25–32, https://doi.org/10.1016/j.ejphar.2019.03.012.

[24] J. Liu, J. Gao, Z. Liang, C. Gao, Q. Niu, F. Wu, L. Zhang, Mesenchymal stem cells and their microenvironment, Stem Cell Res. Ther. 13 (2022) 429, https://doi.org/10.1186/s13287-022-02985-y.

[25] S. Méndez-Ferrer, T.V. Michurina, F. Ferraro, A.R. Mazloom, B.D. Macarthur, S.A. Lira, D.T. Scadden, A. Ma'ayan, G.N. Enikolopov, P.S. Frenette, Mesenchymal and haematopoietic stem cells form a unique bone marrow niche, Nature 466 (2010) 829–834, https://doi.org/10.1038/nature09262.

[26] Z. Tong, Z. Yin, Distribution, contribution and regulation of nestin+ cells, J. Adv. Res. S2090–1232 (23) (2023), https://doi.org/10.1016/j.jare.2023.08.013, 00230–8.

[27] W.-W. Luo, R. Ma, X. Cheng, X.-Y. Yang, Z. Han, D.-D. Ren, P. Chen, F.-L. Chi, J.-M. Yang, Afferent synaptogenesis between ectopic hair-cell-like cells and neurites of spiral ganglion induced by Atoh1 in mammals in vitro, Neuroscience 357 (2017) 185–196, https://doi.org/10.1016/j.neuroscience.2017.05.040.